

Inductive Acceleration of Moving Projectiles and Synchronization between the Driving Field and the Projectile Motion

J. Nett and L. Gernandt

French-German Research Institute of Saint-Louis (ISL)
5 rue du Général-Cassagnou - 68301 SAINT LOUIS CEDEX (France)

Abstract—One of the main problems of multistage induction launchers is the synchronization between the fields of the stator coils and the projectile motion.

Numerical calculations with a simulation code as well as experiments to accelerate projectiles with initial velocities up to 500 m/s, carried out in a small calibre test launcher with a gas gun as preaccelerator and a single electromagnetic stage, showed the importance of the correct timing of the stator coil current in relation to the projectile position and velocity. Some typical test results are reported, discussed and compared with results of numerical simulation.

I. INTRODUCTION

Among the numerous different types of electromagnetic coil guns and launchers, according to the different possible geometries and ways to excite the driving magnetic field and the field connected to the projectile [1], multistage coaxial induction accelerators are one of the most promising groups of systems.

A multistage coaxial induction launcher consists of a number of stationary drive or stator coils placed coaxially along the projectile path. Each of these discrete coils is energized separately when the projectile is located in the right position as it passes through. The current pulse in such a stator coil induces an inversely directed current in a coil attached to the projectile or in the metallic projectile itself. Acceleration occurs, due to the repulsive force between these coil or loop currents in conformity with Lenz's law. In a first approximation this force K is given by

$$K = -\frac{M}{L_p} \cdot i_A^2 \frac{dM}{dx}, \quad (1)$$

where i_A is the current in the drive coil, L_p the inductance of the projectile coil, M the mutual inductance between the two coaxial coils and dM/dx its gradient [2]. This equation (1) shows that a powerful acceleration can only be achieved when the pulsed current in the stator coil becomes high and when at the same time the position of the projectile coil

gives a good coupling (i.e. a high value of M) and also shows a high gradient dM/dx .

Multistage coaxial induction launchers offer several advantages over other electromagnetic accelerators, but they also have their problems and limitations [3]: the advantages, for instance, include the distributed energy storage, the distribution of recoil, the simple geometry and a resulting simplified force containment as well as a high operating efficiency, but the main feature is that there is no need for moving current carrying contacts or brushes. Problems arise from the heating of the projectile coil or the projectile, from the need for fast switches for high currents and voltages and from the necessity of having an exact synchronization between the projectile motion and the timing in order to energize the different stator coils. An improper synchronization reduces not only the thrust in an acceleration stage but also its efficiency.

The present paper deals with the last of these problems. Numerical calculations with a simulation code as well as experiments with a small calibre experimental launcher were carried out in order to study the inductive acceleration on moving projectiles and the synchronization between the timing of the driving field and the projectile motion. A description of the experimental set-up and the simulation code will be given. Some typical test results are reported, compared with results of numerical simulation and discussed.

II. THE LABORATORY COIL ACCELERATOR AND THE EXPERIMENTAL SET-UP

A small calibre multi-purpose laboratory launcher, designed and constructed for system studies, for checking simulation models and codes and for testing coil gun components, was used for the investigations presented in this paper.

This experimental launcher consists (as shown schematically in fig. 1) of a gas gun ① as a preaccelerator, a gas dump tank ②, a section where the electromagnetic acceleration stages under test can be introduced ③, a section to observe the projectile in flight ④ and a tank to stop and catch it up ⑤.

This work has been supported by the Ministry of Defense of the Federal Republic of Germany under contracts BMVg T/R 760/M 0006/M 1706 and T/R 760/N 0001/N 1701.

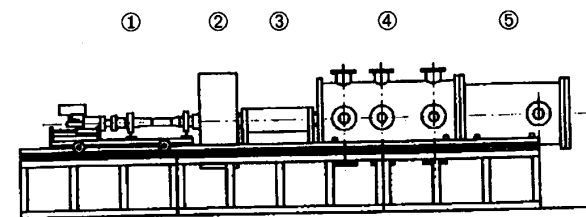


Fig. 1. Schematic view of the laboratory coil launcher (calibre 20 mm)

With the gas gun (calibre 20 mm, max. pressure 200 bar) projectiles with masses of 10 g could be accelerated to velocities up to 450 m/s using helium at a pressure of about 50 bar as driving gas. The dump tank, which surrounds a perforated part of the barrel, is useful for recovering the driving gas and for lowering down the pressure behind the projectile in order to avoid a further increase of velocity due to gasdynamic forces in the electromagnetic acceleration section. For the study presented here, the laboratory launcher was equipped with only one inductive acceleration stage. The gas gun was used to give the projectiles (in a controllable manner) an initial velocity ranging up to 400 m/s before they enter the electromagnetic stage. In this way, it was possible to study the acceleration of moving projectiles and the synchronization of the accelerating field with the projectile motion without being disturbed by the electromagnetic pulse and noise of a preceding stage.

The experimental arrangement in the electromagnetic test section for this study is shown schematically in figure 2.

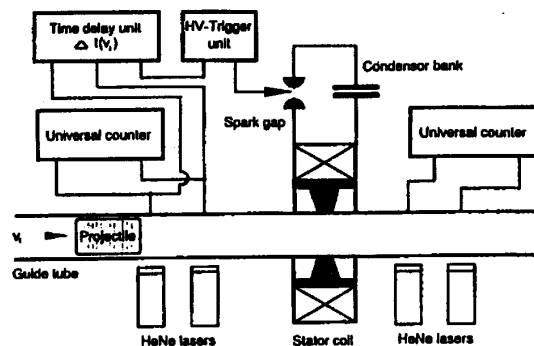


Fig. 2. Block diagram of the experimental arrangement in the electromagnetic acceleration section

A capacitor bank with a peak energy of 20 kJ (capacity of 106 μF ; peak charging voltage 20 kV) and an electrically triggerable three electrode spark gap as switch were used as energy source to power the stator coil. With two double laser light barriers located before and behind this coil and two 10 MHz counters, the initial velocity of the projectile and the velocity after the acceleration process could be

measured. The system in front of the coil was also used to detect the passage of the projectile and to give a synchronization impulse to trigger the spark gap switch via a time delay unit and a high-voltage trigger generator. With a high-voltage probe and a Rogowski coil - not shown in figure 2 - the voltage on the capacitor bank and the current in the stator coil could be measured. In order to avoid disturbances due to electromagnetic noise, all the electronic measuring, recording and control instruments were installed in a Faraday cage and all the test and control signals were transmitted optically into and out of this screened room via optical fibers.

As stator coil a so-called "transformer coil with flux concentrator" was used. This type of coil can be regarded as a combination of a mechanically strong single turn coil with a pulse transformer to match its impedance to the energy source. It consists of a solid cylindrical core with an inner bore and a radial slot (fig. 3). This core, made of a metal of high electrical conductivity, is surrounded by a multiturn coil, which serves as primary coil of a transformer. A current pulse in this primary induces a current of opposite direction into the core which acts as secondary coil. Due to the skin effect, this current flows in a thin layer on the outer surface of the core. By means of the slot it is turned to the inside, where it will flow around the inner contour of the bore in the same direction as the exciting current and where it can be concentrated by using an appropriate geometry of the bore. In this way nearly the total flux of the exciting coil will be concentrated in this part of the bore.

A more detailed description of the principles of operation and construction and of the features of such a coil as well as some results of experiments to accelerate projectiles from rest are given in earlier papers [4, 5].

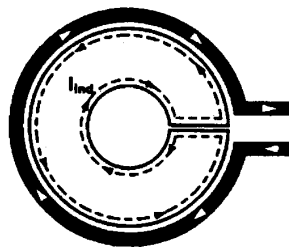


Fig. 3. Principle of a transformer coil (showing primary winding and secondary core with bore and slot)

As projectiles we used aluminium cylinders (Al 6060) with an outer diameter of 20 mm and a length of 25 mm with a bore in the front part to reduce the mass to 10 g.

III. MODEL FOR NUMERICAL SIMULATION OF INDUCTIVE ACCELERATION

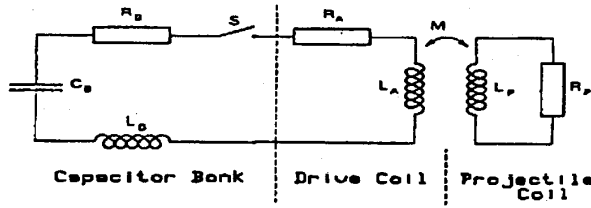


Fig. 4. Equivalent circuit diagram of a single stage of an induction accelerator

Figure 4 shows the lumped parameter circuit of a single stage of an induction launcher. The model we used to simulate the acceleration of the moving projectile in such a stage is based on this circuit and has been described in a former paper [5]. The main difference between this model and comparable ones in the literature [6, 7] is that we use measured values for the mutual inductance and its gradient instead of calculated ones. The numerical simulation program has to solve the mesh equations for the driving circuit (2) and for the projectile circuit (3), the equation (4) which gives the accelerating force K and the equation of motion (5):

$$U_C = U_0 - \frac{1}{C_B} \int_0^t i_A dt = (R_A + R_B) \cdot i_A + (L_A + L_B) \cdot \frac{di_A}{dt} + M \cdot \frac{di_P}{dt} + v \cdot i_P \cdot \frac{dM}{dx} \quad (2)$$

$$0 = R_P \cdot i_P + L_P \cdot \frac{di_P}{dt} + M \cdot \frac{di_A}{dt} + v \cdot i_A \cdot \frac{dM}{dx} \quad (3)$$

$$K = i_A \cdot i_P \cdot \frac{dM}{dx} \quad (4)$$

$$K = m \cdot b = m \cdot \frac{dv}{dt} = m \cdot \frac{d^2x}{dt^2} \quad (5)$$

All the parameters in the driving circuit (charging voltage U_0 ; capacity C_B , resistance R_B and inductance L_B of the capacitor bank; resistance R_A and inductance L_A of the drive coil) are known or can be measured. The experimental method used to determine the mutual inductance M between the drive and the projectile coil and its gradient dM/dx as a function of their distance is also given in the earlier paper [5]. The inductance L_P and the resistance R_P of the projectile coil were calculated with the following expressions (6) and (7) [5]:

$$L_P = \mu_0 \cdot r_P \left[\ln \frac{8r_P}{l_P} - 0.5 \right] [H], \quad (6)$$

$$R_P = \frac{\rho \pi (2r_P - d_{eff})}{l_P \cdot d_{eff}} [\Omega], \quad (7)$$

where μ_0 is the free space permeability, ρ the specific resistivity, r_P the radius, l_P the length of the annular current

carrying part of the projectile and d_{eff} its effective thickness equal to the skin depth $\delta = \sqrt{2\rho / \mu_0 \omega}$ or its geometric thickness d if $d \leq \delta$. Besides the skin effect, the projectile heating and the change of the resistance R_P with temperature were also taken into account. Besides these values for the electrical circuits and the geometry and material of the projectile, its total mass m and its initial velocity v_0 and position x_0 at the moment when the driving current begins to flow must be given.

Then with this program the following parameters can be calculated as a function of time:

- voltage on capacitor bank U_C ,
- current in drive coil i_A ,
- current in projectile coil i_P ,
- temperature of projectile coil T ,
- force on projectile K ,
- acceleration of projectile b ,
- velocity of projectile v ,
- position of projectile x ,
- efficiency of acceleration $\eta = m(v^2 - v_0^2) / C_B U_0^2$.

IV. NUMERICAL AND EXPERIMENTAL RESULTS

In this chapter some significant results obtained with the numerical simulation code and from experiments with the test launcher are presented, compared and discussed. For the computation the same conditions as in the tests (energy source capacity $C_B = 106 \mu F$ and charging voltage $U_0 = 9.7 kV$; projectile mass and material $m = 10 g$ Al 6060) were used, together with the measured or calculated inductances and resistances of the capacitor bank, the drive and projectile coil and the values of the mutual inductance between these coils and its gradient which have been determined with the method described in paper [5].

Figure 5a shows the calculated efficiency η for the acceleration of such a projectile in our test launcher starting from rest as a function of the time t after the beginning of the current flow and as a function of the starting position x_0 in the coil. Figure 5b gives the same relationship for an initial projectile velocity $v_i = 400 m/s$. In both diagrams a marked maximum of the efficiency can be seen. In the case of the projectile starting from rest, this maximum has a value of 0.8% and is situated at the end of the flux concentrator where the mutual inductance M and its gradient dM/dx are both high and give, as shown in equation (1), a high accelerating force. For the initial velocity of 400 m/s this maximum has a value of nearly 3% and the position where this efficiency can be achieved is displaced about 5 mm towards the

central plane of the stator coil. In both diagrams it can be seen that, to get these optimal efficiencies, the position x_0 of

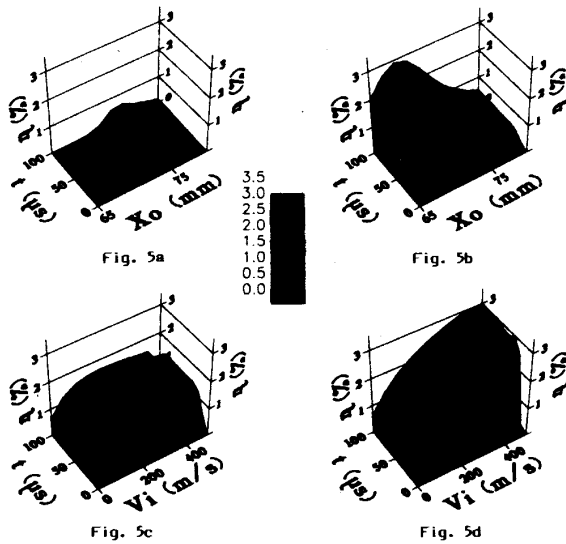


Fig. 5. Calculated efficiency of acceleration in the tested stator coil as a function of time t and as a function of:
a) the initial projectile position x_0 for $v_i = 0$
b) the initial projectile position x_0 for $v_i = 400$ m/s
c) the initial velocity v_i for $x_0 = x_K$
d) the initial velocity v_i for $x_0 = x_{0\text{opt}}(v_i)$

the projectile must be defined with a precision better than ± 1 mm; this means that, at an initial velocity of 400 m/s for example, the timing of the current must be better than ± 2.5 μ s. Figure 5c and d show again the efficiency of acceleration as a function of the time t but now also as a function of the initial velocity v_i in figure 5c for a fixed position x_0 at the end of the flux concentrator; figure 5d shows the same parameters but always for the position where, dependent on the initial velocity, the efficiency becomes optimal. For the fixed position (fig. 5c) the efficiency first increases with the velocity, passes through a maximum at about 250 m/s and is then slightly decreasing, whereas in the case of the optimal position (fig. 5d) it is increasing up to more than 3% for an initial velocity of 500 m/s. These diagrams show that, for the lower velocities, only two half periods of the driving current contribute to the acceleration; for the higher initial velocities only the first half period does.

Besides the simulation results, the first acceleration experiments with moving projectiles within the test launcher also showed the need for a good synchronization in an impressive manner. These experiments were carried out by using the signal of one of the laser light barriers in front of the drive coil delayed with a pulse retarder for a preset delay time in order to trigger the spark gap and to switch on the driving current. Quite small velocity variations of the projectile due to the good but not perfect reproducibility of the gas gun action had a great influence on the electromagnetic

acceleration process. If the velocity was too high, the current pulse came too late to give the projectile a high thrust; if it was too low, then the projectile did not arrive at the accelerating region with a high gradient dM/dx in time and it could be deformed or destructed by radial compression forces developed in the central region of the flux concentrator. Figure 6 shows, on the right, a projectile which was successfully accelerated and, on the left, three projectiles deformed or destructed due to bad synchronization.

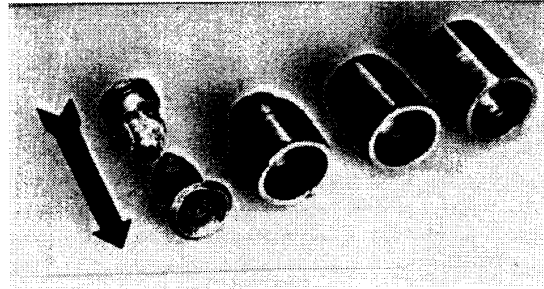


Fig. 6. Picture of accelerated and softly stopped projectiles

To avoid such failures we developed and built a special retarder system which counts the transit time of the projectile between the two laser light barriers in front of the stator coil. By multiplying this transit time with a selected factor corresponding to the ratio of the distance to the desired triggering point inside the drive coil to the distance between the light barriers, the system chooses the correct delay time for triggering the spark gap.

In figure 7 you will find the results of a number of experiments made with the help of this system to accelerate

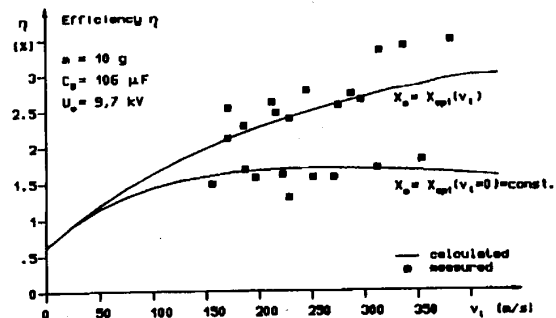


Fig. 7. Comparison of calculated and measured efficiencies of acceleration in the tested stator coil as a function of initial projectile velocity v_i and position x_0

Al 6060 projectiles with a mass of 10 g and initial velocities v_i ranging from 150 to about 400 m/s in a single stage. The energy in the capacitor bank ($C_B = 106$ μ F, $U_0 = 9.7$ kV) was in all cases about 5 kJ. Figure 6 shows the

efficiency of acceleration η , as defined before, according to the initial projectile velocity v_i for two different conditions for the initial projectile position at the onset of the drive current flow:

- for $x_0 = \text{constant}$ and equal to the position at the end of the concentrator where η had its maximum for $v_i = 0$ and
- for $x_0 = x_{\text{opt}}(v_i)$, the position where η had its maximum for the given v_i .

Besides the experimentally obtained points, curves calculated for these conditions with the simulation code are also drawn in figure 6. The good agreement between the experimental point and the theoretical curves shows that, with the retarding and triggering system developed for the inductive test launcher, a good synchronization could be achieved.

V. CONCLUSION AND FUTURE WORK

The experiments to accelerate 20 mm projectiles moving with velocities up to 400 m/s in a single stage reported in the present paper showed that the synchronization between the projectile motion and the energizing of the driving magnetic fields of a coaxial induction launcher is a serious problem, but also showed that this problem could be solved. This is an important fact because the synchronization of high-calibre guns (about 120 to 150 mm) for projectile velocities up to 2 500 or 3 000 m/s needs about the same precision and it should therefore also be possible to make them work.

As the next step in the development of such a gun, we plan to increase the number of stages in our test launcher to study the interaction and electromagnetic compatibility of the different stages.

REFERENCES

- [1] "Coilgun Taxonomy", *Proceedings of the Workshop on Inductive/Coaxial Launchers*, US-Army ARDEC, Picatinny Arsenal/N.J., USA, September 22-24, 1987
- [2] H. Kolm, P. Mongeau, "Basic principles of coaxial launch technology", *IEEE Trans. Magnetics* **MAG-20**, No. 2, p. 227, 1984
- [3] K. McKinney, P. Mongeau, "Multiple stage pulsed induction acceleration", *IEEE Trans. Magnetics* **MAG-20**, No. 2, p. 239, 1984
- [4] H. Nett, L. Gernandt, "Überlegungen und Untersuchungen zum Bau von Antriebsspulen für induktive Spulenbeschleuniger", *ISL report CO 240/89*, 1989
- [5] H. Nett, L. Gernandt, "Inductive acceleration of projectiles with a transformer coil", *Proceedings of the 3rd European Symposium on EML Technology*, London, England, April 16-18, 1991
- [6] P. Raymond, A. Carrière, "Simulation numérique de l'accélération électromagnétique par induction. 1re partie : Boucles filiformes", *ISL report R 102/89*, 1989
- [7] P. Raymond, A. Carrière, "Simulation numérique de l'accélération électromagnétique par induction et premières vérifications expérimentales. 2ème partie : Bobines épaisses", *ISL report R 108/89*, 1989